Report USAFSAM-TR-84-16

MEASUREMENT OF SPECIFIC ABSORPTION RATE IN HUMAN PHANTOMS EXPOSED TO SIMULATED AIR FORCE RADAR EMISSIONS

William D. Hurt, M.S.

June 1984

Final Report for Period October 1980 - September 1981

USAF SCHOOL OF AEROSPACE MEDICINE
Aerospace Medical Division (AFSC)
Brooks Air Force Base, Texas 78235

NOTICES

This final report was submitted by personnel of the Radiation Physics Branch, Radiation Sciences Division, USAF School of Aerospace Medicine, Aerospace Medical Division, AFSC, Brooks Air Force Base, Texas, under job order 7757-01-82.

When Government drawings, specifications, or other data are used for any purpose other than in connection with a definitely Government-related procurement, the United States Government incurs no responsibility or any obligation whatsoever. The fact that the Government may have formulated or in any way supplied the said drawings, specifications, or other data, is not to be regarded by implication, or otherwise in any manner construed, as licensing the holder, or any other person or corporation; or as conveying any rights or permission to manufacture, use, or sell any patented invention that may in any way be related thereto.

The Office of Public Affairs has reviewed this report, and it is releasable to the National Technical Information Service, where it will be available to the general public, including foreign nationals.

This report has been reviewed and is approved for publication.

William D. Hurt
WILLIAM D. HURT, M.S.
Project Scientist

John C. Mitchell
JOHN C. MITCHELL, B.S.
Supervisor

Royce Moser, Jr.
ROYCE MOSER, Jr.
Colonel, USAF, MC
Commander

REPORT DOCUMENTATION PAGE

1a. REPORT SECURITY CLASSIFICATION UNCLASSIFIED	1b. RESTRICTIVE MARKINGS
2a. SECURITY CLASSIFICATION AUTHORITY	3. DISTRIBUTION/AVAILABILITY OF REPORT Approved for public release; distribution is unlimited.
2b. DECLASSIFICATION/DOWNGRADING SCHEDULE	
4. PERFORMING ORGANIZATION REPORT NUMBER(S) USAFSAM-TR-84-16	5. MONITORING ORGANIZATION REPORT NUMBER(S)
6a. NAME OF PERFORMING ORGANIZATION USAF School of Aerospace Medicine 6b. OFFICE SYMBOL (If applicable) USAFSAM/RZP	7a. NAME OF MONITORING ORGANIZATION
6c. ADDRESS (City, State and ZIP Code) Aerospace Medical Division (AFSC) Brooks Air Force Base, Texas 78235	7b. ADDRESS (City, State and ZIP Code)
8a. NAME OF FUNDING/SPONSORING ORGANIZATION USAF School of Aerospace Medicine 8b. OFFICE SYMBOL (If applicable) USAFSAM/RZP	9. PROCUREMENT INSTRUMENT IDENTIFICATION NUMBER
8c. ADDRESS (City, State and ZIP Code) Aerospace Medical Division (AFSC) Brooks Air Force Base, Texas 78235	10. SOURCE OF FUNDING NOS. PROGRAM ELEMENT NO. 62202F; PROJECT NO. 7757; TASK NO. 01; WORK UNIT NO. 82
11. TITLE (Include Security Classification) MEASUREMENT OF SPECIFIC ABSORPTION RATE IN HUMAN PHANTOMS EXPOSED TO SIMULATED AIR FORCE RADAR EMISSIONS	
12. PERSONAL AUTHOR(S) Hurt, William D.	
13a. TYPE OF REPORT Final Report 13b. TIME COVERED FROM Oct 1980 TO Sep 1981	14. DATE OF REPORT (Yr., Mo., Day) 1984, June 15. PAGE COUNT 13
16. SUPPLEMENTARY NOTATION	

17. COSATI CODES		
FIELD	GROUP	SUB. GR.
06	02	
06	18	

18. SUBJECT TERMS (Continue on reverse if necessary and identify by block number)
Radiofrequency radiation; Specific absorption rate; Radiation depth-dose distribution.

19. ABSTRACT (Continue on reverse if necessary and identify by block number)
It has been suggested that pulsed radiofrequency radiation (RFR) fields may produce different specific absorption rate (SAR) distributions than continuous wave (CW) exposures. SAR distributions were measured in a muscle-equivalent slab for various RFR frequencies and duty-cycle combinations. No significant differences in SAR distribution between pulsed and CW were measured.

20. DISTRIBUTION/AVAILABILITY OF ABSTRACT UNCLASSIFIED/UNLIMITED ☒ SAME AS RPT. ☐ DTIC USERS ☐	21. ABSTRACT SECURITY CLASSIFICATION UNCLASSIFIED
22a. NAME OF RESPONSIBLE INDIVIDUAL William D. Hurt	22b. TELEPHONE NUMBER (Include Area Code) (512) 536-3749 22c. OFFICE SYMBOL USAFSAM/RZP

DD FORM 1473, 83 APR EDITION OF 1 JAN 73 IS OBSOLETE.

MEASUREMENT OF SPECIFIC ABSORPTION RATE IN HUMAN PHANTOMS EXPOSED TO SIMULATED AIR FORCE RADAR EMISSIONS

INTRODUCTION

This experiment was designed to investigate the possibility that the average specific absorption rate (SAR) for pulsed radiofrequency radiation (RFR) varies markedly from the SAR for continuous wave (CW) fields. A homogeneous slab of muscle-equivalent material (MEM) was used for making the SAR distribution measurement at 2.07, 2.8, 5.6, and 9.3 GHz (L-, S-, C-, and X-band respectively).

MATERIAL AND METHODS

RFR Exposures

The RFR exposures were performed in an anechoic chamber 3 m x 7 m x 14 m (Emerson and Cummins, Inc.), using a Cober Electronic, Inc., Peak Power Emission Simulator, Model 2852, with standard gain horns. The frequencies used were 2.07, 2.8, 5.6, and 9.3 GHz. The exposure parameters are listed in Table 1. All experiments were conducted in the far field. Radiofrequency power was monitored continuously using a Hewlett-Packard Power Meter, Model 436A. Incident power densities were measured using a Narda Microwave Corp., Broad Band Isotropic RF Monitor, Model 8316, with a probe, Model 8323.

TABLE 1. EXPOSURE PARAMETERS

Frequency (GHz)	Pulse Rate (pps)	Pulse Width (μsec)
2.07	CW	-
2.07	50,000	2
2.8	500	2
5.6	50 and 500	2
9.3	200 and 2000	0.5

Real-Time SAR Determination System

Rate of temperature rise due to absorbed RFR was monitored in real-time using a Vitek Electrothermia Monitor, Model 101, (1,2) with output to a Digital Equipment Corp. computer, Model PDP/1134, through a Digital Equipment Corp. analog-to-digital converter, Model AD11-K. The Electrothermia Monitor (3) has a probe diameter of 1 mm, an absolute accuracy ± 0.05°C, a short-term stability ± 0.01°C, a time constant of 0.2 sec, and an RF-line-heating error of 0.005°C for an RF heating equivalent of 1°C/min. The Electrothermia Monitor was calibrated against a Thermometrics Four-Wire Thermistor Standard, Model S-10, (Serial No. 282), which is traceable to the National Bureau of Standards, and had an uncertainty of 0.0015°C.

Exposure of Homogeneous Slab

A homogeneous muscle-equivalent slab, 8-cm deep, 26-cm high, and 33-cm long, was constructed, using the method of Guy (4). The electrical and physical properties of the muscle-equivalent material are given in Table 2. To provide support with minimal perturbation of the RF field, the slab was contained in a box constructed of 2.5-cm-thick low-density, closed-cell Styrofoam HD 300 (Dow Chemical, Midland, Mich.). The probe was inserted into 1.5-mm O.D. glass capillary tubes and positioned at selected depths through the face of the slab, which was opposite the horn, and the temperature was monitored during RFR exposure at a rate of 100 measurements per sec. A linear least-square fit was then calculated for the purpose of determining the rate of temperature rise (T'). This was then used to calculate the SAR according to the following equation (5):

$$SAR\ (W/kg) = (58.6\ W/kg\ per\ °C/min) \cdot T'\ (°C/min).$$

TABLE 2. ELECTRICAL AND PHYSICAL PROPERTIES OF MEM

Frequency (GHz)	Relative Dielectric Permittivity	Conductivity (S/m)	Density (g/cm^3)	Specific Heat
2.07	47.4	1.95	.97	.84
2.8	45.5	2.43	.97	.84
5.6	41.6	4.64	.97	.84
9.3	37.9	8.73	.97	.84

Exposure duration was less than 30 sec to reduce errors due to thermal conduction. Ample time was allowed between exposures for the temperature in the slab to equilibrate ($\nabla T < 0.04$°C in 40 sec) before proceeding. The SAR distributions were compared to theoretical RFR attenuation equations derived by matching boundary conditions for solutions to Maxwell's equations for a dielectric half-space irradiated by a plane wave.

Taken from Figure 1 and Jordan and Balmain (6) the expression for the E-field in the MEM can be written as:

$$E_m = T \cdot \exp\{-z[(\omega\mu[\omega^2\varepsilon^2 + \sigma^2]^{1/2} - \omega^2\mu\varepsilon)/2]^{1/2}\}$$

$$\cdot \exp\{-jz[(\omega\mu[\omega^2\varepsilon^2 + \sigma^2]^{1/2} + \omega^2\mu\varepsilon)/2]^{1/2}\}.$$

where:

z = distance (m),

f = frequency (Hz),

$\omega = 2\pi f$,

μ = permeability (henry/m),

ε = dielectric permittivity (farad/m),

σ = conductivity (S/m), and

$$T = \frac{2E_o}{1 + c\{[\mu(\varepsilon^2 + \sigma^2/\omega^2)^{1/2} + \mu\varepsilon]/2\}^{1/2}}$$

where:

E_o = peak incident electric field strength (V/m) and

$c = (\mu_o\varepsilon_o)^{-1/2}$ (m/sec).

Thus, the average power deposition expression in W/m^3 is:

$$P = \frac{\sigma E_m E_m^*}{2} = \frac{\sigma T^2}{2}.\exp\{-z[2[\omega\mu(\omega^2\varepsilon^2 + \sigma^2)^{1/2} - \omega^2\mu\varepsilon]]^{1/2}\}.$$

Hence, incorporating the specific mass of muscle, we obtain:

SAR (W/kg) = P/970.

RESULTS

The normalized SAR depth distributions (Figs. 2 through 5) show the comparison between the measured values in the finite slab and theoretical predictions for CW fields in a semi-infinite MEM slab. Tables 3 through 5 present the normalized SAR measurements for various pulse conditions.

TABLE 3. 2.07 GHz SAR VS PULSE PARAMETERS

Depth (cm)	CW	2 μs 50K pps
0	.39 ± .05	.38 ± .10
.1	.39 ± .01	.40 ± .05
.2	.36 ± .02	.35 ± .05
.3	.32 ± .01	.33 ± .04
.4	.28 ± .03	.29 ± .04
.5	.25 ± .01	.27 ± .03
.6	.24 ± .04	.24 ± .04
.7	.23 ± .01	.21 ± .04
.8	.19 ± .02	.19 ± .04
.9	.16 ± .01	.17 ± .04
1.0	.14 ± .02	.15 ± .03
1.1	.12 ± .01	.13 ± .03
1.2	.11 ± .02	.12 ± .03
1.3	.097 ± .01	.11 ± .05
1.4	.081 ± .01	.093 ± .03
1.5	.068 ± .01	.084 ± .04

TABLE 4. 5.6 GHz SAR VS PULSE PARAMETERS

Depth (cm)	.5 μs 200 pps	2 μs 50 pps	.5 μs 2000 pps	2 μs 500 pps
0	.71 ± .41	.61 ± .38	.94 ± .06	.98 ± .06
.1	.53 ± .30	.78 ± .30	.90 ± .04	.94 ± .04
.2	.52 ± .36	.56 ± .43	.77 ± .10	.78 ± .12
.3	.49 ± .34	.54 ± .57	.73 ± .11	.71 ± .09
.4	.38 ± .33	.25 ± .32	.51 ± .02	.50 ± .02
.5	.25 ± .41	.12 ± .34	.36 ± .06	.35 ± .03

TABLE 5. 9.3 GHz SAR VS PULSE PARAMETERS

Depth (cm)	.5 μs 200 pps	2 μs 50 pps	.5 μs 2000 pps	2 μs 500 pps
0	1.08 ± .15	1.12 ± .16	1.34 ± .27	1.49 ± .24
.1	1.20 ± .23	1.24 ± .20	1.12 ± .17	.96 ± .26
.2	.78 ± .16	.85 ± .17	.83 ± .13	.80 ± .17
.3	.60 ± .16	.59 ± .20	.59 ± .12	.58 ± .21
.4	.48 ± .15	.38 ± .12	.38 ± .07	.38 ± .07

The uncertainties do not overlap in only two columns in the tables: 5.6 GHz for 0.1 cm with 0.5 μs and 200 pps vs. 2 μs and 500 pps, and 9.3 GHz at the surface with 0.5 μs and 200 pps vs. 2 μs and 500 pps.

The relative dielectric permittivity (ε_r) and conductivity (σ) values used in the derivations of the SAR depth distribution for CW were taken from analytic expressions fit to data for muscle (7). The resulting equations are:

$$\varepsilon_r = 4.3 + \frac{38.1}{1+(f/24)^2} + \frac{11.5}{1+(f/1.9)^2} \quad \text{and}$$

$$\sigma = .92 + \frac{.336f^2}{1+(f/1.9)^2} + \frac{.0884^2}{1+(f/24)^{+2}} \quad .$$

where f = frequency (GHz). This was in lieu of actual measured values of the electrical properties for MEM.

For all of the frequencies used, the SAR measurements near the surface were less than the predicted values. This bias might be due to the effect of surface cooling.

The bias in the data compared to the theoretical predictions (Figs. 2 through 5) may be due to uncertainties in the incident power density measurements. The Narda probe calibration accuracy is ± 12%. Table 6 presents the relative dielectric permittivity and conductivity values which produce the best fit for assumed power densities of 0.9, 1.0, and 1.1 mW/cm^2.

TABLE 6. PARAMETERS FOR BEST FIT

	σ(S/m)			ε_r		
Power density	0.9	1.0	1.1	0.9	1.0	1.1
Frequency						
2.07 GHz	2.1	2.4	2.7	49	65	83
2.8	2.5	2.8	3.2	55	71	92
5.6	3.2	3.7	4.2	23	31	40
9.3	7.7	8.9	10	41	55	70

For the 2.07-, 2.8-, and 9.3-GHz exposures it appears that the incident power density was ~ 10% less than that indicated by the Narda radiation monitor. The data also suggested that the field was ~ 10% greater for 5.6 GHz. However, the measurements agree with theory.

CONCLUSION

The data demonstrate that the average SAR does not depend significantly on pulse parameters for pulse widths as short as 0.5 μs and peak-to-average ratios as large as 10,000:1.

REFERENCES

1. Burr, J. G., D. K. Cohoon, E. L. Bell, and J. W. Penn. Thermal response model of a simulated cranial structure exposed to radiofrequency radiation. IEEE Trans Biomedical Engineering BME-27(8):452-460 (1980).

2. Burr, J. G., and J. H. Krupp. Real-time measurement of RFR energy distribution in the Macaca mulatta head. Bioelectromagnetics 1:21-34 (1980).

3. Bowman, R. R. A probe for measuring temperature in radiofrequency-heated material. IEEE Trans Microwave Theory Tech MTT-24(1):43-45 (1976).

4. Guy, A. W. Analysis of electromagnetic fields induced in biological tissue by thermographic studies on equivalent phantom models. IEEE Trans Microwave Theory Tech MTT-19(2):205-214 (1971).

5. Durney, C. H., M. F. Iskander, H. Massoudi, S. J. Allen, and J. C. Mitchell. Radiofrequency radiation dosimetry handbook, third edition. USAFSAM-TR-80-32, Aug. 1980.

6. Jordan, E. C., and K. G. Balmain. Electromagnetic waves and radiating systems. Englewood Cliffs, N.J., Prentice-Hall, Inc.:1968.

7. Durney, C. H., C. C. Johnson, P. W. Barber, H. Massoudi, M. F. Iskander, J. L. Lords, D. K. Ryser, S. J. Allen, and J. C. Mitchell. Radio-frequency radiation dosimetry handbook, second edition. USAFSAM-TR-78-22, May 1978.

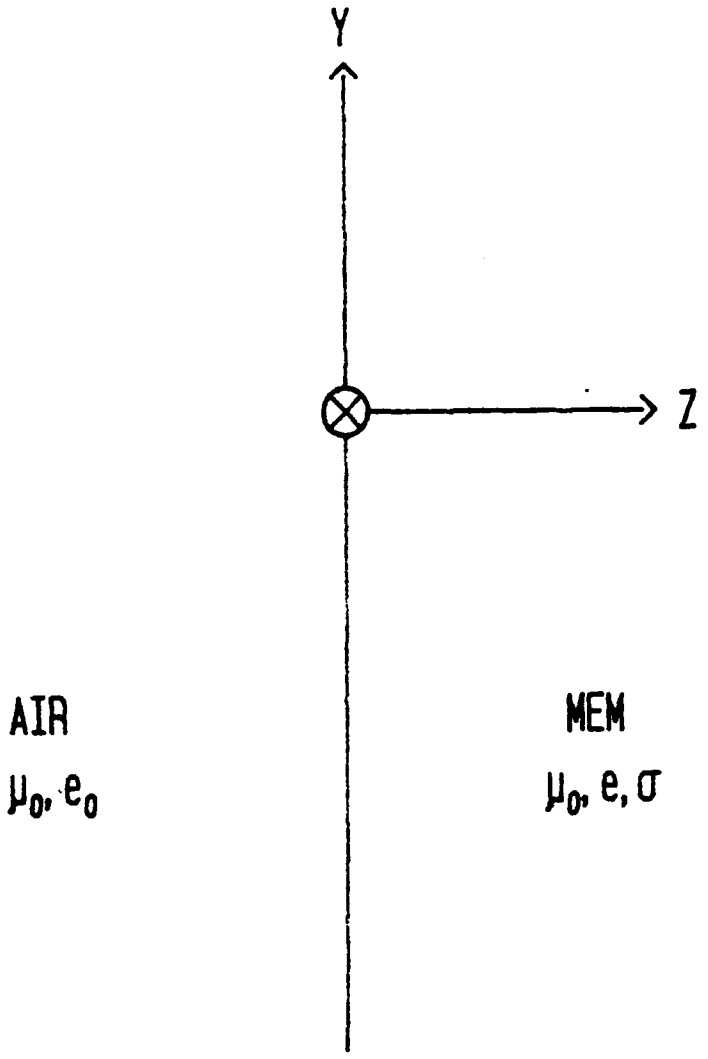

Figure 1. Schematic of semi-infinite space, semi-infinite muscle-equivalent material with indicated coordinate system and electrical parameters.

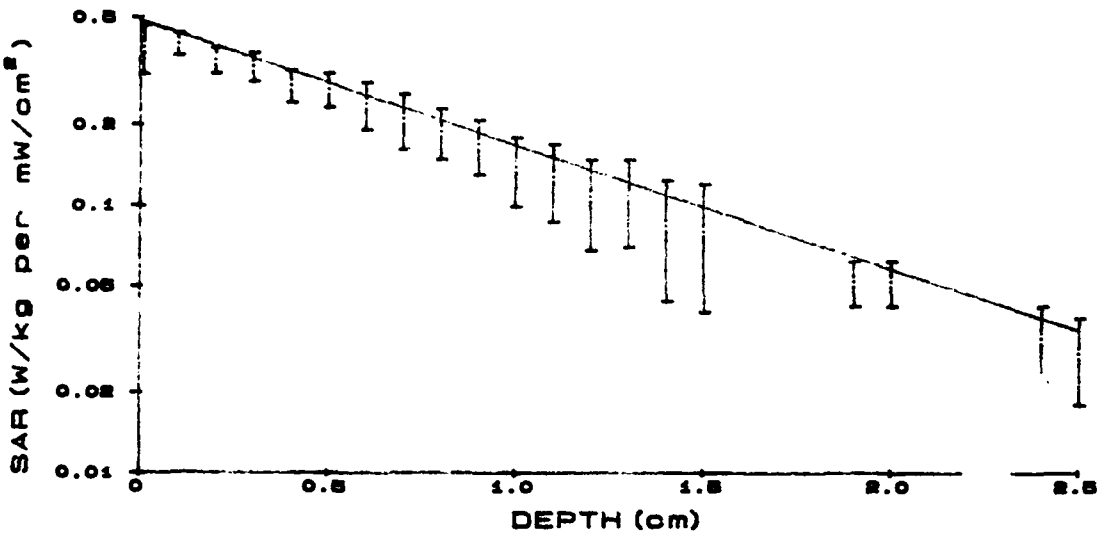

Figure 2. Theoretical SAR distribution and measurements for L-band (2.07 GHz) frequency.

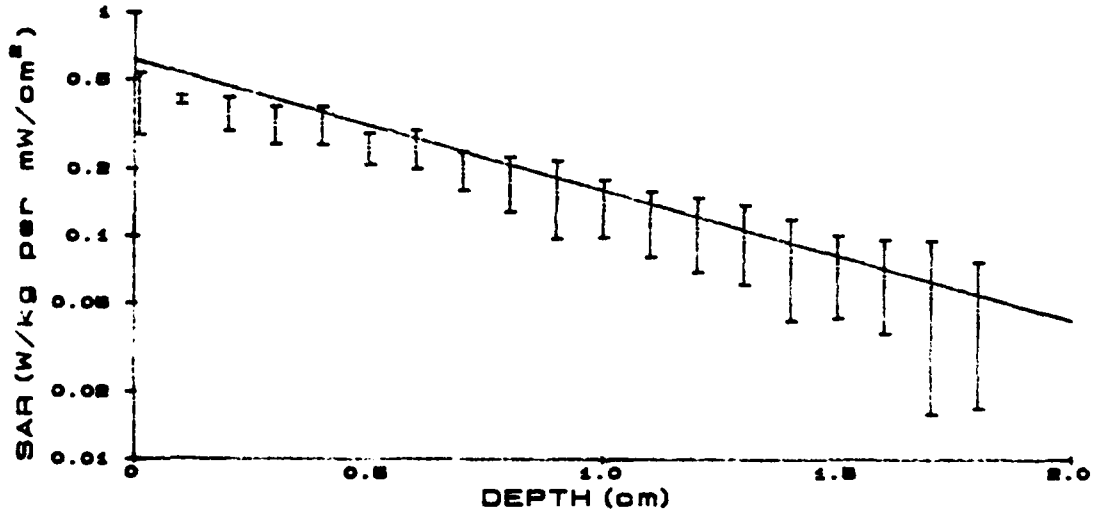

Figure 3. Theoretical SAR distribution and measurements for S-band (2.8 GHz) frequency.

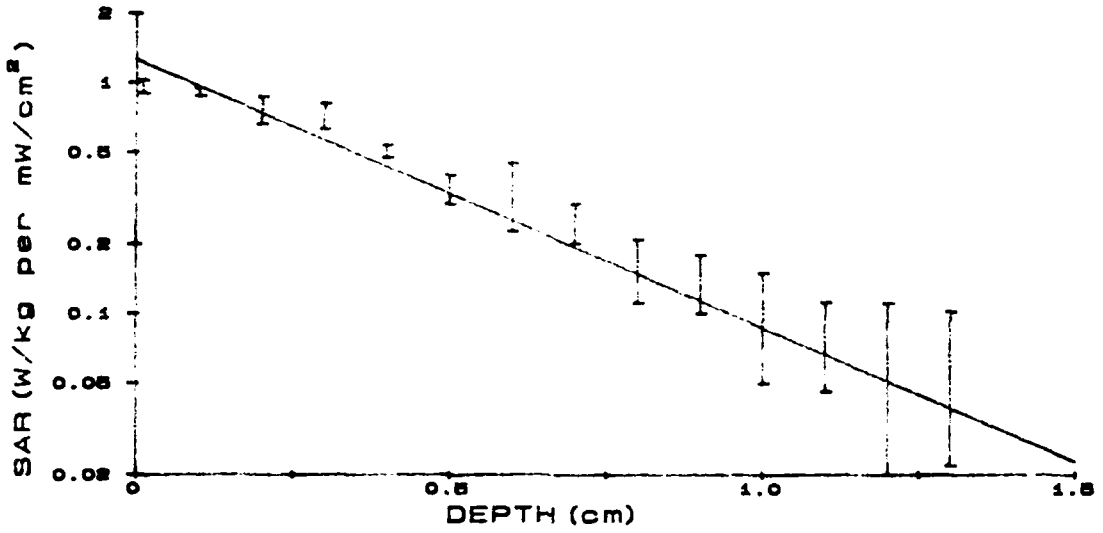

Figure 4. Theoretical SAR distribution and measurements for C-band (5.6 GHz) frequency.

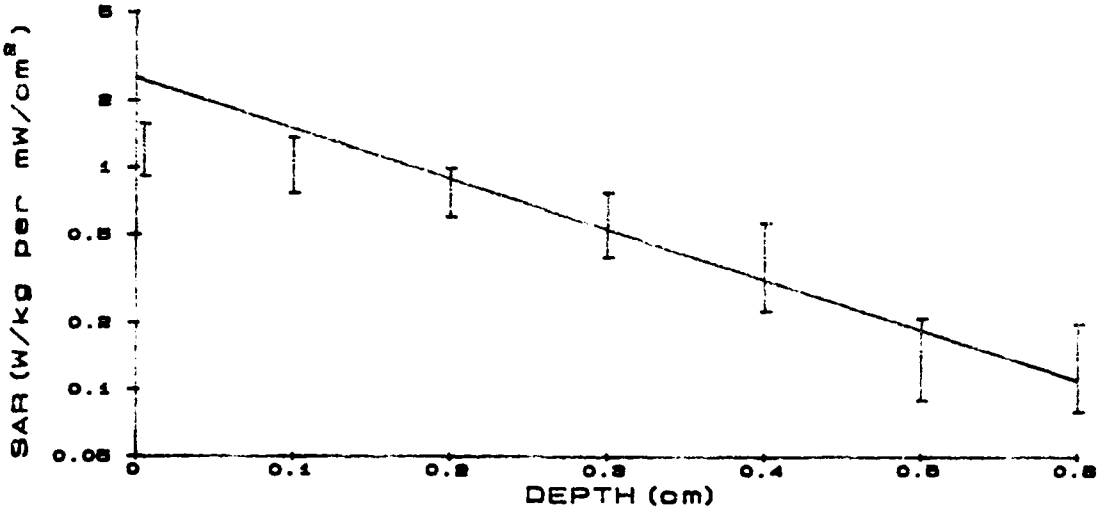

Figure 5. Theoretical SAR distribution and measurements for X-band (9.3 GHz) frequency.